Universidade de Brasília - UnB
Faculdade UnB Gama - FGA
Cursos de Engenharia Automotiva e Aeroespacial

Topology optimization: Application in a hinge support for a Pratt & Whitney PW1000G nacelle casing

Autores: Bruno Vieira Clemente e Isaac Moura de Alencar

Orientadora: Prof. Dra. Carla Anflor

Brasília, DF

2023

Bruno Vieira Clemente e Isaac Moura de Alencar

Topology optimization: Application in a hinge support for a Pratt & Whitney PW1000G nacelle casing

Monografia submetida ao curso de graduação em Engenharia Automotiva e Aeroespacial da Universidade de Brasília, como requisito parcial para obtenção do Título de Bacharel em Engenharia Automotiva e Aeroespacial

Orientadora: Prof. Dra. Carla Anflor

Brasília, DF
2023

I

- A ficha catalográfica oficial deverá ser solicitada à Biblioteca pelo aluno após a apresentação.

Topology optimization: Application in a hinge support for a Pratt & Whitney PW1000G nacelle casing

Bruno Vieira Clemente e Isaac Moura de Alencar

Monografia submetida como requisito parcial para obtenção do Título de Bacharel em Engenharia Automotiva e Aeroespacial da Faculdade UnB Gama - FGA, da Universidade de Brasília, em 16/02/2023 apresentada e aprovada pela banca examinadora abaixo assinada:

Prof. Dra.: Carla Tatiana Mota Anflor, UnB/ FGA
Orientador

Prof. Dr.: Sergio Henrique da Silva Carneiro, UnB/ FGA   Membro Convidado

Prof. Dra.: Maria Alzira de Araújo Nunes, UnB/ FGA   Membro Convidado

Brasília, DF
2023

AGRADECIMENTOS

RESUMO

O surgimento de técnicas avançadas de fabricação, como a fabricação aditiva de metais, tem possibilitado a produção de peças com geometrias cada vez mais complexas. Quando combinadas com softwares de Engenharia Assistida por Computador (CAE) e Análise de Elementos Finitos (FEA), os projetistas podem otimizar os componentes para sua função pretendida. O impacto dessas técnicas é particularmente significativo em indústrias em que o peso é um fator crítico de desempenho, como as indústrias aeroespacial, astronáutica e automotiva. Nas indústrias aeroespacial, astronáutica e automotiva de alto desempenho, o peso dos componentes é mais crítico do que o custo de fabricação. Este estudo tem como objetivo demonstrar a eficácia do método *Solid Isotropic Material with Penalization* (SIMP) na redução do peso de componentes aeroespaciais sem comprometer a segurança. Será desenvolvida uma abordagem passo a passo, que pode ser aplicada a uma ampla gama de geometrias para reproduzir os resultados alcançados neste estudo. Os resultados obtidos neste trabalho podem servir como ponto de partida para análises posteriores, como fadiga, crescimento de trincas, modal, simulações de fabricação aditiva e outros. Assim, o estudo demonstra a validade da otimização topológica como estratégia para reduzir o peso de componentes aeroespaciais e lança as bases para pesquisas futuras.

Palavras-chave: Otimização topológica. Método SIMP. Análise de Elementos Finitos (FEA). Engenharia Assistida por Computador (CAE). Manufatura aditiva. Aeroespacial. Automotivo.

ABSTRACT

The emergence of advanced manufacturing techniques, such as metal additive manufacturing, has enabled the production of parts with increasingly intricate geometries. When combined with Computer-Aided Engineering (CAE) and Finite Element Analysis (FEA) software, designers can optimize components for their intended function. The impact of these techniques is particularly significant in industries where weight is a critical performance factor, such as aerospace, astronautic, and automotive industries. In high-performance aerospace, astronautics, and automotive industries, the weight of components is more critical than their manufacturing cost. This study aims to demonstrate the effectiveness of the Solid Isotropic Material with Penalization (SIMP) method in reducing the weight of aerospace components without compromising their safety. A step-by-step approach will be developed, which can be applied to a broad range of geometries to reproduce the results achieved in this study. The results obtained in this research can serve as starting points for further analyses, such as fatigue, crack growth, modal, additive manufacturing simulations, and others. Thus, the study demonstrates the validity of topological optimization as a strategy to reduce the weight of aerospace components and lays a possible foundation for future works.

Keywords: Topology optimization. SIMP method. FEA. CAE. Addictive manufacturing. Aerospace. Automotive.

LISTA DE FIGURAS

LISTA DE TABELAS

LISTA DE SÍMBOLOS

S - Skewness

A - Area of the element

L - Perimeter of the element

C - Tabled constant for element quality

F - Deformation gradient tensor

$V0$ - Volume of the element in the undeformed configuration

JdV - Volume of the element in the deformed configuration

d - Material density

p - Penalization exponent

B_i - Strain displacement matrix for the i-th element

K_{ij} - Stiffness matrix for the i-th element

λ - Relaxation factor

C - Compliance

SUMÁRIO

1 INTRODUCTION

Topology optimization is a mathematical method used to design structures or materials with optimal performance using the least amount of material possible. It is a powerful tool for aerospace and automotive engineering, as it allows engineers to design structures and components that are both strong and lightweight, which is crucial for achieving efficiency and performance in these fields.

In aerospace engineering, topology optimization is used to design aircraft structures such as wings and fuselages, propulsion systems, and other components. By using topology optimization, engineers can design aircraft that are more efficient, have greater range, and are able to withstand the high loads and stresses of flight.

In automotive engineering, topology optimization is used to design various components, such as chassis and suspension systems, engines and transmissions, and body structures. Using topology optimization, engineers can design more fuel-efficient cars that have better performance and are safer to drive.

Overall, topology optimization has significantly impacted aerospace and automotive engineering by enabling the design of stronger, more efficient, and more cost-effective structures and components. It is a powerful tool that helps engineers to make better use of materials and improve performance, which has the potential to lead to significant advances in these fields.

1.1 SELECTION OF THE PIECE

With the theme chosen, the subsequent logical step was its implementation. In this decision-making process, two challenges were encountered. The first challenge was identifying a suitable piece that pertained to both automotive and aerospace engineering, and the second challenge was verifying the validity of any results obtained through the optimization of said piece. Despite the first challenge not being entirely overcome, the second challenge was addressed by utilizing the methodology established in the article by Tomlin (2011) and comparing the results obtained in this thesis with those presented in Tomlin's study.

As previously argued, even though the selected piece is derived from the field of aviation, the methodology and results obtained are still pertinent to any engineering industry, albeit potentially for different applications or reasons.

1.2 MOTIVATION

In the aeronautical industry, the weight of an aircraft directly affects its operating costs through increased fuel consumption, which in turn leads to higher CO_2 emissions. According to ICAO Doc 10013 4.1.2, the fuel burn for additional weight on board an aircraft is typically 2.5 - 4.5 % of the additional weight per hour of flight, depending on the aircraft's characteristics (Tabernier, 2022).

The potential environmental impact of weight reduction can be clearly demonstrated through the results of the weight reduction of 10 kg on food carts used by All Nippon Airways (ANA). According to ANA (2021), the new lightweight cart has achieved a weight reduction of up to 10 kg compared to the conventional cart, resulting in a weight reduction effect of approximately 580 kg per Boeing 777-300ER aircraft. This reduction in weight leads to a significant reduction in fuel consumption, estimated to be approximately 5,700 tons annually. This reduction in fuel consumption, in turn, results in a reduction of CO_2 emissions equivalent to that of approximately 17,500 25 m swimming pools. This serves as a clear illustration of the potential environmental impact of weight reduction in the aviation industry.

The aviation industry has demonstrated its commitment to environmental sustainability through the pledge and plans of the International Air Transport Association (IATA) to achieve net zero carbon emissions by 2050. This commitment, as stated by IATA (2021), serves as a clear indication of the industry's dedication to reducing its environmental impact and addressing the issue of climate change.

In the automotive industry, weight plays a critical role in fuel efficiency and CO_2 emissions. As stated by Addere (2021), "reduction in weight can help improve fuel and energy efficiency, and also the carbon emissions from the vehicle as a whole." This highlights the importance of weight reduction in the automotive industry, not only for economic reasons but also for environmental reasons. Additionally, it has been observed that luxury auto manufacturers are increasingly using titanium despite its elevated cost, as reported by Addere (2021). This further emphasizes the significance

of weight reduction in the automotive industry as luxury manufacturers are willing to incur higher costs to achieve it.

1.3 OBJECTIVE

The main goal of this work relies on replicating the research conducted by Tomlin & Meyer (2011) within the constraints of using Ansys's student license. The student license restricts meshing to a maximum of 120,000 nodes. Using Tomlin's results as comparison, creating a method that could be employed for optimizing other geometry. The primary challenge that will be encountered is the lack of essential data such as technical drawings and boundary conditions. This deficiency of information is likely a result of market confidentiality restrictions imposed by either Boeing or Pratt & Whitney.

This thesis is structured into five chapters. In this first chapter the motivations behind this thesis, an overall contextualization of topology optimization in the current market and the objectives were presented.

The second chapter serves as an introduction to the subjects of study and provides a scientific background for the methodology used in the subsequent chapter.

The third chapter details the steps taken by the authors, the challenges encountered during the research process, and the strategies employed to overcome them.

The fourth chapter presents the results obtained using the methodology outlined in the previous chapter, along with a comparison of these results to those obtained by Tomlin & Meyer.

In the fifth and final chapter, the previous chapters are summarized and commented on, and suggestions are made for how this work could be used as a basis for future research.

2   THEORETICAL FOUNDATION

2.1   THE FINITE ELEMENT METHOD

The finite element method (FEM) is a powerful numerical technique used to analyze the behavior of structures under various loading conditions. It is a widely used method in structural engineering, as it allows for analyzing complex structures subjected to complex loading conditions.

In the FEM, a structure is divided into small interconnected elements, which can be analyzed individually and then assembled to predict the overall behavior of the structure. The elements used in the analysis can be one-dimensional (1D), two-dimensional (2D), or three-dimensional (3D), depending on the complexity of the structure and the loading conditions.

One of the key advantages of the finite element method is its ability to capture the local behavior of a structure. According to Cook, Malkus, Plesha, and Witt. (1989), "the finite element method is particularly well-suited for analyzing structures with complex shapes, such as those with thin or thick-walled sections, or with abrupt changes in geometry." By dividing the structure into small elements, it is possible to accurately capture the local behavior of the structure, which can be difficult to predict using other methods.

In addition to considering the size and shape of the elements, it is also important to consider the material properties of the structure and the loading conditions. The material properties are typically represented using a stiffness matrix, which describes the material's response to external loads. The loading conditions are applied to the elements using nodal forces, which represent the forces acting on the nodes of the elements.

To solve the behavior of the structure using the FEM, it is necessary first to define the stiffness matrix and nodal forces for each element. Then, the stiffness matrix and nodal forces are assembled into a global stiffness matrix and global nodal forces, respectively. The global stiffness matrix and global nodal forces can then be used to solve the nodal displacements of the structure using a system of equations.

Overall, the finite element method is a powerful tool for predicting the behavior of structures under various loading conditions. By carefully considering the size and

shape of the elements, as well as the material properties and loading conditions, it is possible to obtain accurate and reliable results from the analysis.

2.2   DEGREES OF FREEDOM IN THE FINITE ELEMENT METHOD

Degrees of freedom (DOF) play a crucial role in static structural finite element analysis, representing the number of independent displacements or rotations that can be applied to a structure. In other words, they represent the number of ways in which a structure can move or deform under external loads.

A structure can be divided into several small, interconnected elements, each with a set of nodal points. Each nodal point is assigned a certain number of degrees of freedom, which determines the type of movement that can occur at that point. For example, a nodal point may have three degrees of freedom for translations (displacements in the x, y, and z directions) and three degrees for rotations (around the x, y, and z axes).

It is essential to carefully consider the degrees of freedom when performing static structural finite element analysis, as the accuracy of the analysis depends on the correct representation of the structure's movements. The International Association for Shell and Spatial Structures, "the degree of freedom at each node should be determined by the type of element, the loads acting on the structure, and the boundary conditions."

After determining the degree of freedom at each nodal point, it is also necessary to consider the overall degree of freedom of the structure. A structure's total degree of freedom is the sum of the degree of freedom at each nodal point, and it must be equal to the number of independent loads applied to the structure. Suppose the total degree of freedom does not equal the number of independent loads. In that case, the structure is considered indeterminate, and additional calculations are needed to determine the forces and displacements at each nodal point (REDDY 2006).

2.3   ELEMENT TYPES

In static structural finite element analysis, element types refer to the various types of elements that can be used to model a structure. These elements are used to divide the structure into small, interconnected pieces, each of which can be analyzed separately to determine the forces and displacements at each nodal point.

Many different element types can be used in finite element analysis, including beam elements, shell elements, and solid elements. Each type of element is suited to a specific type of structure or load case, and the choice of element type can significantly impact the accuracy of the analysis.

Shell elements are used to model thin-walled structures, such as plates and shells, that are subjected to in-plane and out-of-plane loads. These elements have a larger number of degrees of freedom, typically eight or more, and are well-suited for modeling structures with complex geometries.

Solid elements are used to model three-dimensional structures, such as solids and shells with thickness, that are subjected to all six degrees of freedom of motion (three translations and three rotations). These elements have the highest number of degrees of freedom and are well-suited for modeling structures with complex geometries and loads.

In addition to these basic element types, there are also specialized elements available for specific types of structures or load cases, such as cable elements for modeling tension-only members and contact elements for modeling contact and friction between structural elements.

It is important to carefully consider the element type when performing static structural finite element analysis, as the choice of element can greatly impact the accuracy of the analysis (FREY; GEORGE, 2008).

2.3.1 3D element types

According to Zienkiewicz and Taylor (2000), "three-dimensional elements are used to model bodies which may be subjected to torsion, bending, and/or shear." These elements are useful in analyzing statically determinate structures, where the forces and displacements can be determined through the application of equilibrium equations. Examples of statically determinate structures include trusses, frames, and simple shear walls.

One type of 3D element commonly used in the finite element method is the brick element, also known as the "eight-node solid element." This element has eight nodes, or points of connection, and is defined by eight corner points and the corresponding nodal degrees of freedom. The element stiffness matrix is derived using the

displacement method, and the element stresses and strains are obtained using the constitutive equations of the material. Figure (1) shows some examples of brick elements.
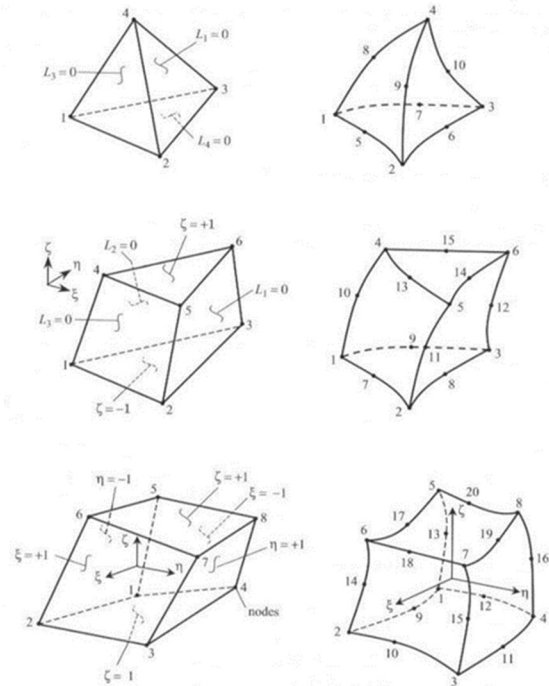
Figure 1. Linear and quadratic tetrahedral, prism and brick elements. (Reddy, 2006)

Another 3D element commonly used in the finite element method is the tetrahedron element, also known as the "four-node solid element." This element has four nodes and is defined by four corner points and the corresponding nodal DOFs. The element stiffness matrix is derived using the finite element shape functions, and the element stresses and strains are obtained using the constitutive equations of the material.

In addition to these standard 3D elements, more specialized elements are available for specific types of structures or loads. For example, the "thick-shell element" is often used to analyze thin-walled structures, such as pressure vessels or aircraft fuselages.

The use of 3D elements in the finite element method allows for a more accurate analysis of statically determinate structures, particularly those subjected to lateral loads. According to Cook, Malkus, Plesha, and Witt (1989), "the use of three-dimensional solid elements provides a more accurate representation of the structural

behavior, particularly in the case of shear and torsion." By capturing these effects, 3D elements can provide valuable insight into the behavior and performance of these structures.

Overall, the choice of element type in the finite element method depends on the complexity of the structure and the accuracy required in the analysis. 3D elements are particularly useful in the analysis of statically determinate structures subjected to lateral loads, as they can capture the effects of shear and torsion on the structure.

2.3.2 Solid 187 Element

The SOLID 187 element, as mentioned in the Ansys help page, is a widely used element in linear static and dynamic analyses of solid bodies. It is a 3D, 10-node, linear hexahedral element, which means it has ten nodes with three degrees of freedom at each node: translations in the nodal x, y, and z directions. This element is noteworthy for its advanced capabilities, including plasticity, hyperelasticity, creep, stress stiffening, large deflection, and large strain, which allow for the simulation of complex material behavior. Additionally, it has the capability for mixed formulation, which is useful for simulating the deformations of nearly incompressible elastoplastic materials, and fully incompressible hyperelastic materials. Finally, this element is useful for analyzing structures with high deformation or inelastic behavior. Figure (2) exemplifies the general geometry of the element type.
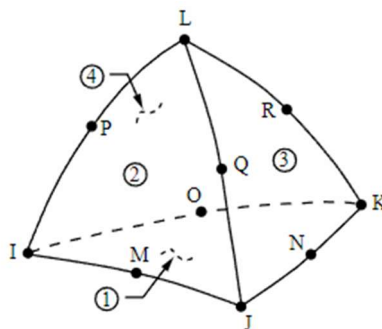
Figure 2. Solid 187 geometry. Ansys (2023)

It is important to note that the SOLID 187 element is chosen to be used in the analysis discussed in the article. Based on the properties previously discussed, the

SOLID 187 element was suitable for the topology optimization analysis presented in the thesis.

2.4   MESH GENERATION

Overall, the choice of the element type in the finite element method depends on the complexity of the structure and the accuracy required in the analysis. For example, 3D elements are useful in analyzing statically determinate structures subjected to lateral loads, as they can capture the effects of shear and torsion on the structure.

Several types of meshes can be used in finite element analysis, including structured meshes, unstructured meshes, and hybrid meshes. Each type of mesh has unique characteristics and is suited to a specific type of structure or load case.

Unstructured meshes are grids of elements arranged in a more flexible, irregular pattern. These meshes are more flexible and can be used to model structures with complex geometries, but they may require more time and effort to generate and may not be as accurate as structured meshes. Nevertheless, according to Reddy (2006), "unstructured meshes are particularly useful for analyzing problems with complex geometry, as they offer a high level of flexibility and adaptability."

Hybrid meshes are grids of elements that combine structured and unstructured meshes. These meshes offer the flexibility and adaptability of unstructured meshes with the accuracy and efficiency of structured meshes and are well-suited for analyzing structures with both simple and complex geometries. According to Hughes, Francfort, and Bazilevs (2005), "hybrid meshes offer a good balance between accuracy and efficiency and are particularly useful for analyzing problems with both simple and complex geometry."

It is important to carefully consider the type of mesh when performing static structural finite element analysis, as the choice of mesh can greatly impact the accuracy and efficiency of the analysis.

2.4.1 Mesh quality metrics

Mesh quality metrics are measures of the quality and effectiveness of the mesh used in static structural finite element analysis. These metrics are used to evaluate the resolution, accuracy, and efficiency of the mesh, and they can help to identify problems or potential issues with the mesh.

The quality of the mesh, or arrangement of elements, plays a critical role in the accuracy and efficiency of the analysis. Therefore, it is important to consider various mesh quality metrics when creating a finite element model.

2.4.1.1 Aspect ratio

One commonly used mesh quality metric is the aspect ratio of an element. The aspect ratio is defined as the ratio of the longest element edge to the shortest element edge. According to Reddy (2006), "elements with high aspect ratios tend to have distorted shapes and may produce inaccurate results." Therefore, it is generally desirable to have elements with low aspect ratios.

2.4.1.2 Skewness

Another commonly used mesh quality metric is the skewness of an element. The skewness of an element is a measure of how much the element deviates from a regular shape, such as a triangle or a quadrilateral. Elements with high skewness tend to produce less accurate results and may require more computational resources.

One way to quantify skewness is using the skewness measure, S represented in Eq. (1):

$$S = \left[\frac{4A}{L^2}\right]^{\frac{1}{2}}$$

(1)

Where A is the area of the element and L is the perimeter of the element. A value of S close to 1 indicates a well-shaped element, while a value of S significantly greater than 1 indicates a highly skewed element. Figure (3) shows the difference between highly skewed triangles and quadrilaterals and their ideal equilateral and equiangular forms.
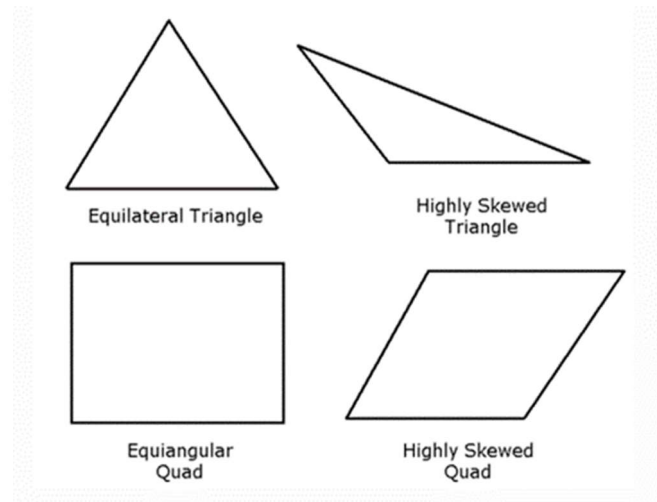
Figure 3. Differentiates between highly skewed triangles and quadrilaterals and their ideal equilateral and equiangular forms. (ANSYS, 2023)

2.4.1.3 Element quality

Another commonly used metric is the "element quality". This metric is based on the ratio of the volume to the sum of squared edge lengths for 2D quad/tri elements or the square root of the cube of the sum of squared edge lengths edges for 3D elements. A value of 1 indicates a perfect cube or square, while 0 indicates that the element has zero or negative volume. The value for the element quality can me calculated as shown in Eq. (2):

$$Quality = C \frac{VOLUME}{\left(\sqrt{(\sum Edgelenght)^2}\right)^3}$$

(2)

Where C is a tabled constant. Table (1) lists the value of C for different types of elements.

Table 1 – Values of C for different element types (ANSYS 2022).

Element	Value of C
Triangle	6.92820323
Quadrangle	4.0
Tetrahedron	124.70765802
Hexahedron	41.56921938
Wedge	62.35382905
Pyramid	96

2.4.1.4 Jacobian ratio

The Jacobian ratio, also known as the Jacobian determinant, is defined as the ratio of the volume of an element in the deformed configuration to the volume of the same element in the undeformed configuration. It is denoted by "J" and is given by the Eq. (3):

$$J = det(F) = \left(\frac{1}{V0}\right) * \iint JdV$$

(3)

Where $det(F)$ is the determinant of the deformation gradient tensor F, $V0$ is the volume of the element in the undeformed configuration, and $\iint JdV$ the volume of the element in the deformed configuration. (ANSYS, 2023).

The Jacobian ratio is a measure of element distortion and can be used to assess the quality of a finite element mesh. A value of 1 indicates that the element has not distorted during deformation, while values less than 1 indicate contraction, and values greater than 1 indicate expansion. A good finite element mesh should have Jacobian ratios close to 1, indicating minimal distortion of the elements. This can be achieved by using appropriate element shapes and sizes through mesh refinement in regions of high deformation.

2.5 TOPOLOGY OPTIMIZATION

Topology optimization is a technique used in static structural finite element analysis to optimize the shape and structure of a design to improve its performance under a given set of loads and constraints. This technique involves using optimization algorithms to iteratively alter the geometry of the structure to minimize its weight or maximize its stiffness while still satisfying the necessary constraints and design requirements.

Topology optimization can be used to optimize a wide range of structures, including beams, trusses, and shells, and it can significantly improve a design's performance and efficiency. According to Sigmund (2013), "topology optimization has the potential to revolutionize the design process by allowing engineers to automatically generate optimal designs that are lighter, stronger, and more efficient."

Several types of topology optimization algorithms can be used in finite element analysis, including density-based optimization, level set optimization, and evolutionary optimization. Each algorithm has unique characteristics and is suited to a specific structure or optimization challenge.

Density-based optimization algorithms use a design variable, such as material density, to represent the optimized structure. These algorithms iteratively alter the density of the structure to minimize the weight or maximize the stiffness while still satisfying the necessary constraints and design requirements.

Level set optimization algorithms involve using a continuous function, known as the level set function, to represent the boundary of the optimized structure. These algorithms iteratively alter the boundary of the structure to minimize the weight or maximize the stiffness while still satisfying the necessary constraints and design requirements.

Evolutionary optimization algorithms involve using a population of design candidates, evolved through selection, mutation, and recombination. These algorithms iteratively alter the design candidates to minimize the weight or maximize the stiffness while still satisfying the necessary constraints and design requirements.

Tomlin's article proposes a methodology similar to that of Seabra et al. (2016). The methodology proposed by Seabra et al. includes steps for fabricating the optimized piece through addictive manufacturing, and its steps can be visualized in Fig. (4).
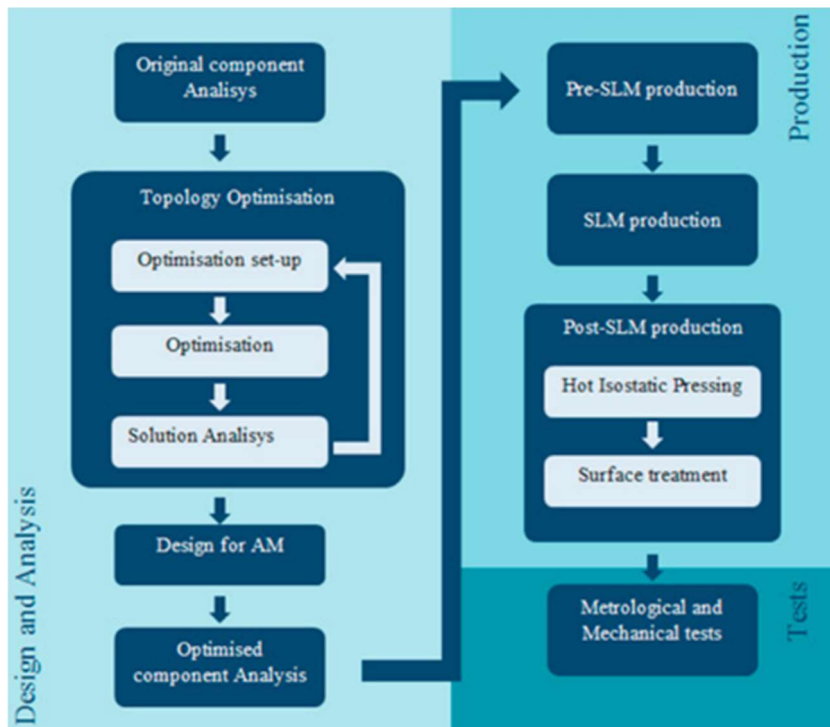
Figure 4. Methodology scheme. Seabra et al. (2016).

2.5.1 The SIMP method

The SIMP (Solid Isotropic Material with Penalization) method is a widely used topology optimization algorithm that involves the use of a design variable, known as material density, to represent the structure being optimized. This method is based on penalizing the structure's stiffness by reducing the material density in regions where the material is not needed while still maintaining the necessary structural integrity and strength.

The SIMP method can be used to optimize a wide range of structures, including beams, trusses, and shells, and it has the advantage of being relatively simple to implement and easy to understand. According to Sigmund (2013), "the SIMP method is a popular and well-established topology optimization algorithm that has been widely used in various structural optimization problems."

The basic steps of the SIMP method are as follows:

1. Define the optimization problem: This involves specifying the design variables (material densities), the objective function, the constraints

(structural integrity, strength, etc.), and the design domain (geometry of the structure).

2. Iteratively update the material densities: This involves using an optimization algorithm, such as the method of moving asymptotes (MMA), to iteratively update the material densities to minimize the objective function while satisfying the constraints.

3. Check for convergence: This involves checking whether the optimization algorithm has converged to a satisfactory solution or whether additional iterations are needed.

4. Post-process the results: This involves analyzing the final design, including the distribution of material densities and the resulting structural behavior, to assess the performance and efficiency of the optimized structure.

The SIMP method can be expressed mathematically as follows:

Objective function:

$$minimize: F \ = \ \Sigma \ (1 - d)^p \ * \ f(x)$$

(4)

Where d is the material density, p is the penalization exponent, and $f(x)$ is the stiffness at each element (BENDSOE; SIGMUND, 2003).

The penalization exponent p for metals is 3. For nonmetallic materials a study must be performed in order to obtain the value of p.

The SIMP method uses an iterative algorithm to solve this optimization problem. At each iteration, the material density of each element is updated based on the sensitivity of the compliance with respect to the material density. The sensitivity is calculated using Eq. (5):

$$\frac{\delta C}{\delta x_i} = \ p \ * \ x_i^{p-1} \ * \ C \ + \ \sum (B_i \ * \ K_{ii} \ * \ B_i^T)$$

(5)

Where B_i is the strain-displacement matrix for the i-th element and K_{ij} is the stiffness matrix for the i-th element.

The material density of each element is then updated using Eq. (6):

$$x_{i(new)} = \max\left(x_{min}, \min\left(x_{max}, x_{i(old)} * \left(1 - \lambda * \frac{\frac{\delta C}{\delta x_i}}{C}\right)\right)\right)$$

(6)

Where "λ" is a positive constant known as the relaxation factor.

The relaxation factor controls the rate at which the optimization process moves towards the desired solution. It is used to balance the trade-off between satisfying the constraints of the problem (such as compliance and volume fraction) and minimizing the objective function (such as the weight or compliance per unit volume). The value of the relaxation factor can be adjusted during the optimization process to improve the convergence of the solution. Typically, a value between 0.8 and 0.9 is used as a starting point.

The SIMP method continues until the compliance has been minimized to the desired level or the maximum number of iterations has been reached.

3 METHODOLOGY

In this chapter the procedures employed for the nacelle support optimization analysis are introduced.

As previously mentioned, the object of study selected was a nacelle support for maintenance purposes, which bears the weight of the casing. Figure (5) shows an example of the chosen geometry being used.
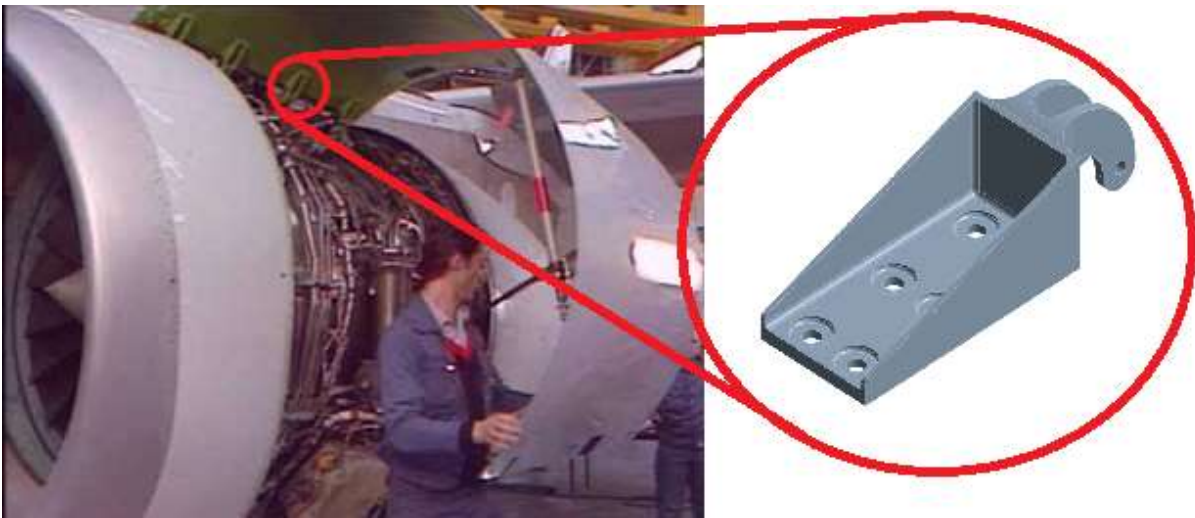
Figure 5. Example of the mounting of the nacelle casing support. Unknown author adapted.

Software from the Ansys Workbench was used, such as Ansys SpaceClaim and Ansys Mechanical, with the extra help of AutoDesk Fusion for preliminary geometry design. Ansys Workbench was used to model the necessary analysis and to define the material. A preliminary CAD was created in the Fusion software from AutoDesk and then exported to the Workbench used as the initial geometry. SpaceClaim was used to simplify the geometry, removing rounded corners and other superfluous parts in the analysis. SpaceClaim was also used to smoothen the geometry obtained from the topology optimization procedure. Finally, Mechanical was used to run the static structural and topology optimization analysis and obtain the results. Figure (6) illustrates how a Workbench tree for topology optimization would look like.

Figure 6. Example of topology optimization Workbench tree.

A work schematic was created with guidelines to the optimization procedure. As seen in figure (7), the first step is the creation of the first geometry. The geometry is subsequently analyzed and optimized. The results of each analysis is used as the basis for the following geometries until satisfactory results are obtained.
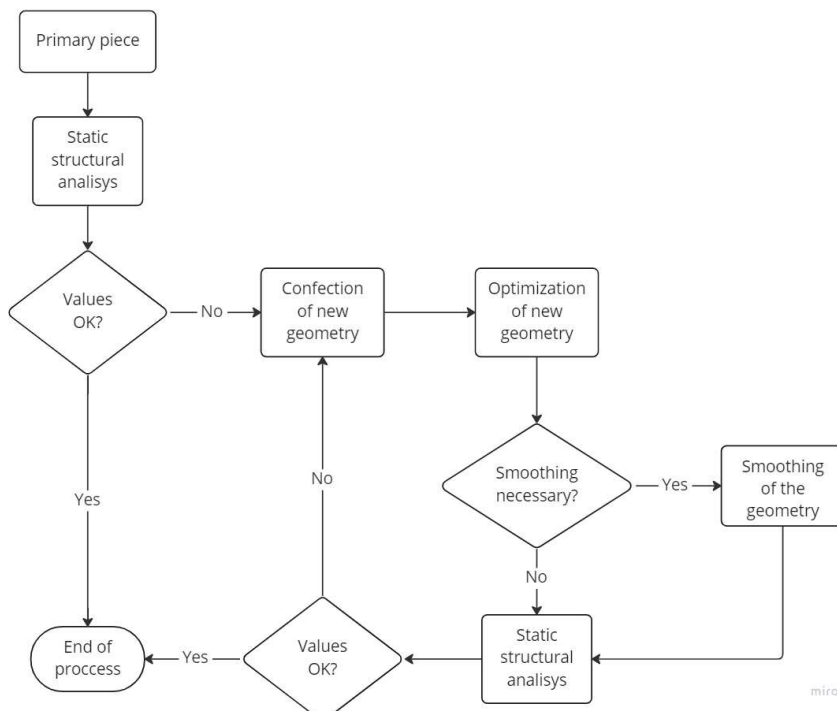
Figure 7. Overall steps taken in the methodology.

3.1 GEOMETRY DESIGN

The initial geometry was based on the model created by Tomlin (2011) and the images disposed are shown in Fig. (8).
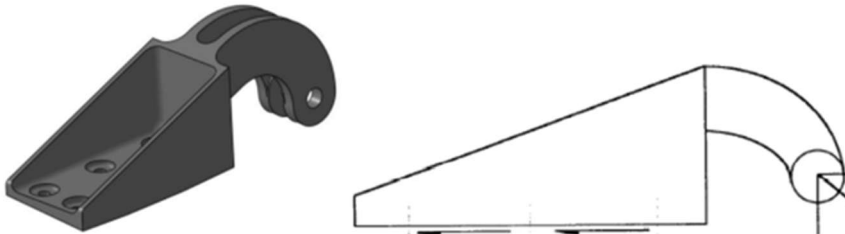
Figure 8. Sketched obtained of the pre optimized piece (TOMLIN 2011).

The lack of information is justified by reasons of patent and technological advances, given that the article developed by Airbus is not in the interest of having competitors have easy access to the same material. Due to the lack of quotas and views that would allow for a more faithful design, an adaptation was made according to the available views after several attempts until a satisfactory result was found.

The first geometry obtained is shown in Fig. (9). Note that this is the unaltered version of the geometry, yet to be simplified for meshing purposes, reducing the number of nodes and elements. This geometry has a mass of 440.33 grams, a value that will be used for comparison in the results section.
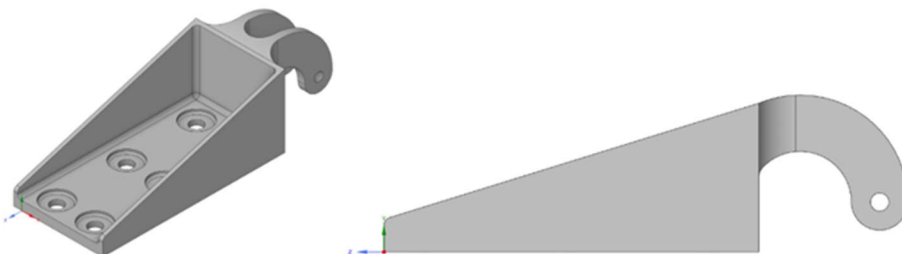
Figure 9. Reproduced CAD by the authors.

A second geometry was created, resembling a cuboid form for structural analysis, followed by a topology optimization to understand how the geometry would

behave during optimization under the same boundary conditions. Many studies use the same principle, starting from a simplified geometry to analyze the behavior of the optimization, as seen in Song Yuejiao Wang (2019), Mitchell's studies shown by Silva (2001), and Abbey (2017), among others. Figure (10) shows the views of the geometry that was used.
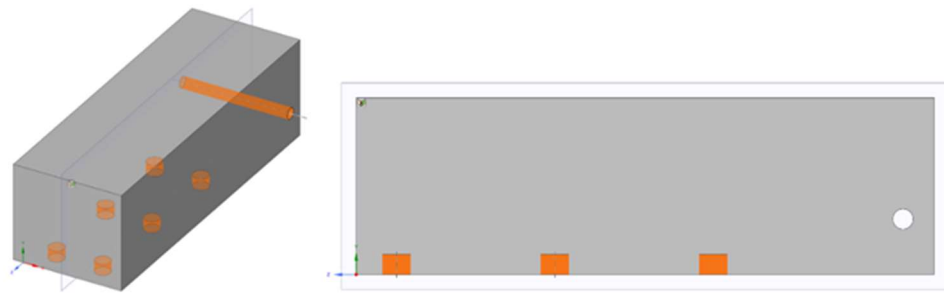
Figure 10. Isometric and lateral view of the filled piece.

Table (2) shows a comparison of the properties of the geometric configurations between the two created geometries.

Table 2 - Dimensions of the created geometries.

Geometry	Original	Cuboid
Length (mm)	55.00	55.00
Width (mm)	47.56	48.16
Height (mm)	157.57	157.57
Volume (mm^3)	5.7186e+004	4.1454e+005

3.2 MATERIALS

Material selection was based on Tomlin's (2011) work. For the support previously used by the company, HC 101 steel was used, which is part of the ferrous steels of the stainless and heat-resistant steel groups mainly composed of chrome, nickel, copper, and molybdenum. For the printed parts, the titanium alloy TI-6Al-4V was used, which is one of the most widely used materials in additive manufacturing in the aerospace and automotive industry, as seen in chapter 1, due to its low density and high values for resistance, mainly composed of titanium, aluminum, and vanadium.

The data is presented in this thesis using the lowest values in order to make a conservative analysis, given that the same material may have different values. The data for the TI-6Al-4V alloy was taken from the work itself. Due to the lack of information about Poisson's ratio presented in Tomlin's work, the data was found on the AZO website. As an alternative, the data found for the titanium alloy was taken from the Ansys library instead of the TI-6Al-4V used by Tomlin.

Table (3) shows some of the obtained material properties.

Table 3 Selected material properties

Material	HC 101 steel	Ti-6Al-4V	Titanium alloy
Density (g/cm^3)	7.7	4.42	4.62
Poisson's ratio	0.3	0.31 ~ 0.37	0.36
Elasticity module (GPa)	193	116	96
Yield stress (MPa)	800	1,008	930
Ultimate tensile strength (MPa)	950	1,085	1,070

The main goal is to reduce the weight of the piece, resulting in long-term cost savings, the used titanium alloy has a lower density, so only by changing the material would an improvement in the structure's mass be noticeable.

Using titanium alloy, a material widely used in additive manufacturing of metals with higher ultimate tensile levels than HC 101, the freedom of design can be explored, thus producing parts that would be impossible or not feasible by conventional manufacturing methods such as casting and machining.

3.3 MESH

The process of discretization makes it essential to create a mesh with good quality, with the lowest number of nodes and elements possible, in order to avoid unnecessary computational costs. Therefore, several parameters were tested for mesh generation, and minimum values were set for Element Quality, a mesh metric used to measure the quality of the model, and a maximum value for the number of nodes and elements.

When analysis time is considered, it is necessary to find a middle ground between mesh quality and the number of elements, combining a quality that can have validated results with a reasonable analysis time for daily applications.

An average of 0.75 for the element quality metric was set as a minimum while also considering the other metrics described in chapter 2. Standard deviation was also noted as a parameter to keep an eye on.

The factor considered for the analysis time is the number of nodes and mesh elements generated. Since the mesh also depends on its quality, a maximum limit of 120,000 elements was stipulated, the maximum value that can be used with the free student license provided by Ansys.

The generation of the Ansys Mechanical standard mesh uses approximately 8 mm as a maximum element size, returning distorted elements, so it is necessary to redo the obtained mesh. A good way to do this refinement is to take half of the smallest edge of the geometry as the standard value for each element, forcing the software to create a more detailed mesh. Another way would be to use the adaptive mesh size with higher resolutions, creating an automatic mesh of higher quality.

After a few meshes were created, the authors decided not to use the "resolution" option, which can be set from a value between 0 and 7, with 7 generating smaller mesh elements than the previous ones. Instead, the chosen option was to define a set value in millimeters for the element size, with adaptative sizing turned off and capture curvature turned on. Tab. (4) shows some of the meshes that were taken into consideration for the initial geometry combined with values for the element quality.

Table 4 – Obtained mesh properties for the initial geometry.

Mesh Element Size (mm)	Mesh Average	Mesh Standard Deviation	Mesh Nodes	Solution MAPDL Elapsed Time [s]
10	0.6832	0.1526	19,345	3
9	0.6842	0.1510	19,655	4
8	0.6906	0.1473	20,351	3
7	0.6988	0.1450	21,038	3
6	0.7086	0.1400	22,508	3
5	0.7275	0.1322	25,341	3
4	0.7604	0.1241	31551	4
3	0.7986	0.1145	47264	5
2	0.8070	0.1041	106249	8

Analyzing the obtained results makes it possible to verify that the maximum element size of 2 mm is optimal for the analysis when considering average quality, standard deviation, and elapsed time. Even with almost double the time spent using 3 mm as a maximum element, the choice of using 2 mm can be justified due to the simplicity of the CAD, resulting in only 8 seconds of computing time.

Given the constraints of a limited number of nodes in the student license and a maximum value of 1 for element quality, it is stipulated that the minimum average element quality value should be set at 0.75. This value offers a balance between obtaining accurate results and ensuring that the meshing of a complex geometry remains feasible within the limitations of the student license. While this value is close to the maximum value of 1, it allows for a degree of flexibility in meshing complex geometries, thus ensuring that the results obtained are reliable and of good quality.

Mesh convergence analysis will be displayed alongside the results in chapter 4.

Figure (11) shows the meshed geometry with the defined parameters.
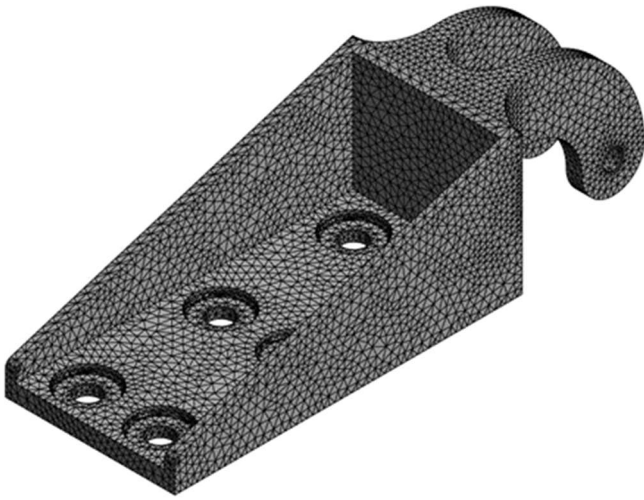
Figure 11. Generated mesh for the piece.

3.4 STATIC STRUCTURAL ANALYSIS

According to Tomlin (2011), it is possible to visualize the stresses subjected to each support. Two cases were studied, but the second was used as a comparison model for the results obtained before and after topological optimization. In this way, it is inferred that the first case returns lower stresses that are less important than the second case. Figure (12) shows an indicator of the supports and the applied forces proportionally.
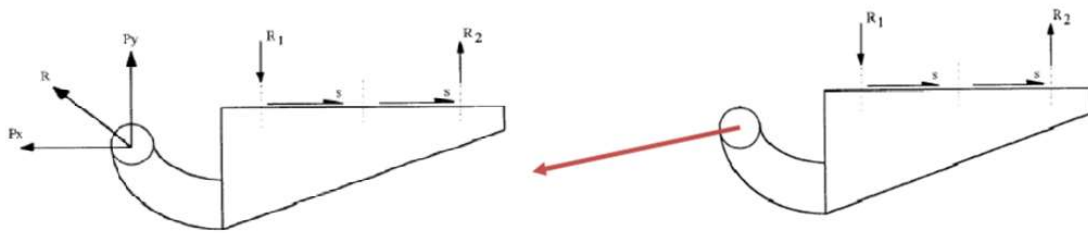
Figure 12. Loading case number one and two respectively (Tomlin, 2011)

The following arrangement was used in Mechanical to perform the analyses: the six holes shown on the base of the piece were used as cylindrical supports, simulating their fixation on the aircraft fuselage, and two remote forces were inserted in the two equidistant holes located at the rear of the piece to simulate the action of the forces described by Tomlin (2011). The values for the two loading cases can be seen in Tab. (5).

25

Table 5 – Loading cases considered in the problem.

Load case	Load X (N)	Load Y (N)	Load Z (N)
1	0	-900	-900
2	0	230	-2300

Given the challenges regarding the dimensions and values already mentioned in the article, the forces were selected following the opposite path since the article provides the results for stress. The values were then adjusted so that the stresses corresponded to those obtained in Tomlin and Meyer (2011). The resultant of the forces in case 1 was 1272.8 N, and for case 2, it was 2311.5 N.

Figures (13) show the cases that were solved in Ansys.
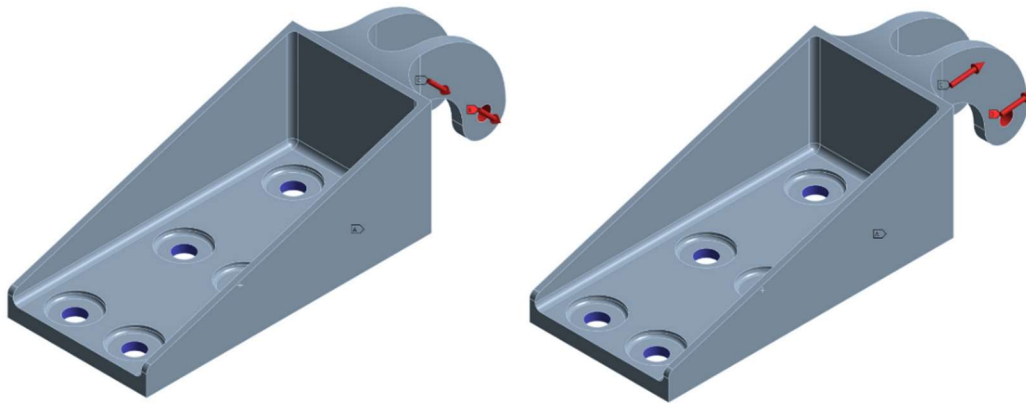
Figure 13. Cylindrical supports and remote forces applied in case number one and case number two.

3.5 TOPOLOGY OPTIMIZATION

Based on the results obtained in the previous static structural analysis and using them as boundary conditions, it is possible through topological optimization to find a geometry with overall better characteristics, such as lower mass and more evenly distributed stresses.

One of the challenges in this case is that the raw result of the topological optimization of the component may not provide useful information, as the original piece is already compact and the optimization program will only remove material from the sides. To better understand the optimization result, a structural analysis and topological

26

optimization of a "filled" piece was performed, as depicted in Figure 26, to visualize the less requested parts of the geometry. During this step, other geometries were evaluated through experimental analyses to determine which one would be the best fit for the geometry found as a solution in the base article.

Another challenge in this case is the absence of design requirements from Airbus and Pratt & Whitney. It is assumed that the company has imposed restrictions, particularly during optimization, on areas of the component that cannot be altered or removed. Due to these restrictions, it is unlikely that an exact reproduction of the result obtained in the base article can be achieved. The focus, therefore, is shifted towards reducing the mass the stress acting on the component.

During the topological optimization process, specific parts of the geometry can be designated as exclusion zones, thereby excluding them from the optimization process. Initially, the areas where the boundary conditions were applied were chosen as exclusion zones in order to maintain the primary features of the component. Additionally, it is possible to determine the quantity of material to be removed as a variable percentage ranging from 0% to 100%, to be selected based on the specific requirements of the project. The optimization process was conducted using two loading cases for all the analyzed geometries, with the excluded regions depicted in Figure (14).
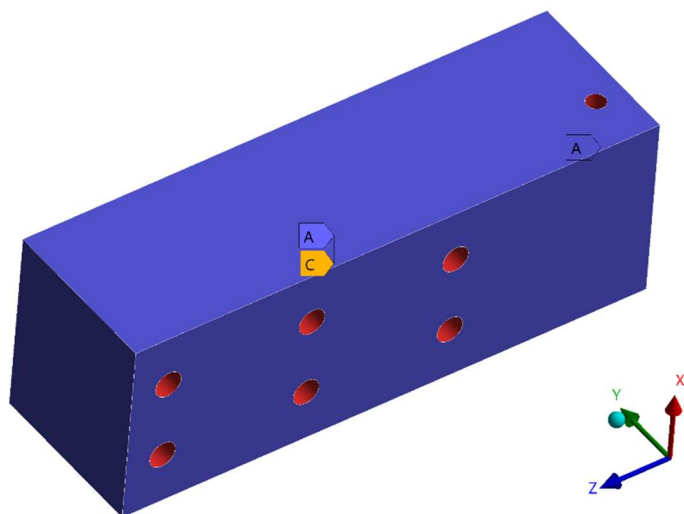
Figure 14. Exclusion zones for the topology optimization cycle of the filled piece.

3.6   GEOMETRY SMOOTHING

The output of the topology optimization process is often a rough, complex geometry that cannot be meshed or manufactured. A post-processing step known as geometry smoothing is often performed to address this issue. This involves taking the rough geometry back to a CAD program such as SpaceClaim and using splines or other techniques to smooth out the rough edges and create a more feasible geometry that can be used for further static analysis or fabrication. Geometry smoothing is an essential step in the design process, as it helps to create a more practical and viable design that can be more easily manufactured and analyzed.

This part is summarized mainly in manual work, starting from sketches of each of the faces of the geometry, using splines to create a more regular geometry.

4   RESULTS

4.1   STATIC ANALYSIS OF THE ORIGINAL GEOMETRY

4.1.1   Tomlin's initial geometry

The first step in creating the topological optimization was to estimate the values for the boundary conditions used by Tomlin (2011). According to Tomlin (2011), Figure (15) shows us the value obtained for the von Mises stress in the primary piece, thus identifying its maximum stress and the relevant points where the structure is most requested.
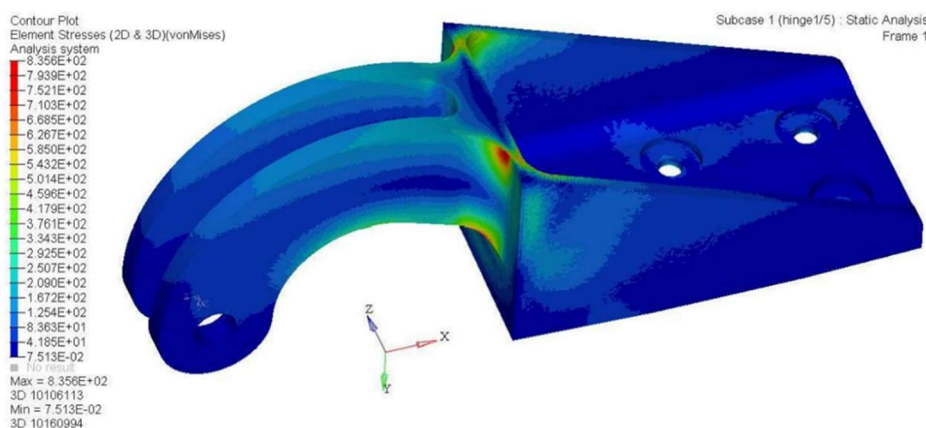
Figure 15. Equivalent (von-Mises) Stress for the initial piece. (TOMLIN, 2011).

4.1.1.1 Mesh metrics

As stated in chapter 2, the following mesh metrics were considered when choosing the mesh for the geometry. The chosen mesh used 2 mm as the maximum element size, and Tab. (6) shows each value.

Table 6 – Mesh metrics obtained for the initial geometry.

Mesh Metric	Mesh Average	Standard Deviation
Element Quality	0.8070	0.1041
Skewness	0.2654	0.1352
Jacobian Ratio	0.9905	0.0473
Aspect Ratio	1.9254	0.5105

4.1.1.2 Static structural analysis

It is possible to infer from the behavior of the structure that there are four well-defined points of maximum stress, all located at the end of the handle that connects it to the front side of the piece, and the value is close to 835 MPa. It is also possible to see that such stress passes through to the other side of the piece, requesting the inner part near the cavity where the holes are located. Considering that the original piece was made of HC 101 steel, whose yield stress is 800 MPa, we have a safety coefficient for von Mises of approximately 0.96, thus expecting structural failure over time. In the lower part of the handle, considerable stresses are also found near 400 MPa, but returning a safety coefficient of approximately 2.0. Some stresses between 250 MPa and 300 MPa are found near the maximum stress values and in the upper part of the handle.

Figures (16) and (17) show the Von Mises values obtained for the created geometry.
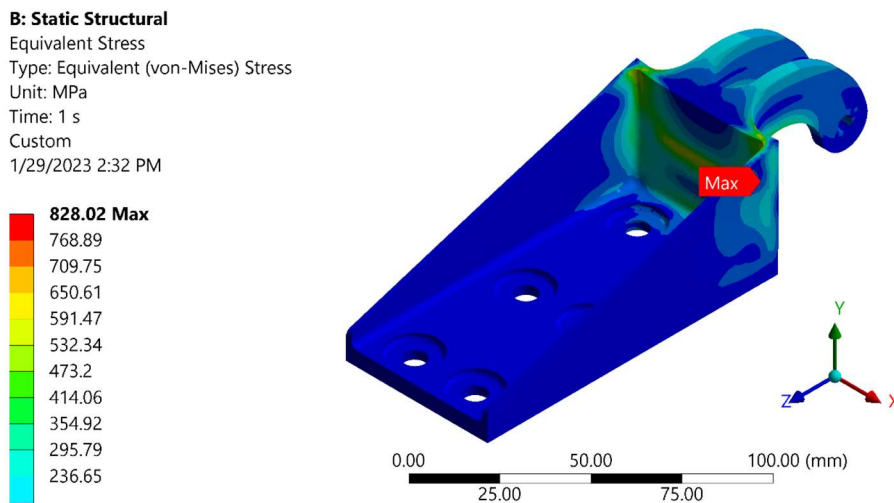
Figure 16. Isometric view of the Equivalent Stress for the original designed piece.
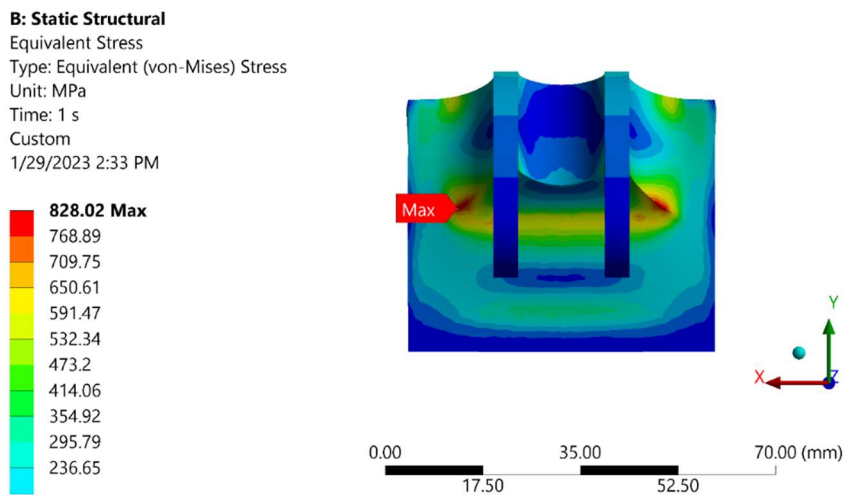
Figure 17. Back view of the Equivalent Stress for the original designed piece.

Observing Fig. (16) and (17), it is possible to notice that the points of maximum stress coincide in the two structures with similar values. The maximum stress is 828.02 MPa, located at the ends of the upper and lower parts of the junction of the handle with the rest of the piece. The safety coefficient found is approximately 0.97 at the most requested points, making the geometry also subject to a potential failure. The remainder of the object exhibits similar behavior to the original, allowing Tomlin's static analysis to be accurately reproduced, resulting in an expected value that can be used to compute the forces in subsequent calculations.

4.1.1.3 Mesh convergence

Another possible approach to demonstrate mesh convergence is to use the "convergence" tool by selecting one of the possible results requested in the solution. The tool starts with an initial mesh with results (for Von Mises stress in this case) and refines it each time a solution is calculated if the desired percentage of maximum change is not achieved. The percentage for the analysis in question was 3%, meaning a new solution would be generated for results that changed more than 3% from the previous result.

The Ansys user manual states, "You can control the relative accuracy of a solution in two ways. You can use the meshing tools to refine the mesh before solving, or you can use convergence tools as part of the solution process to refine solution results on a particular area of the model." (ANSYS, 2023). The criteria used in this thesis were meshing tools and metrics. Nevertheless, the convergence tool mentioned above was also used in this section to ensure accuracy due to license relation limitations.

Table (7) and Fig. (18) show the obtained results.

Table 7 – Convergence tool data from the geometry analysis.

Solution Number	Equivalent Stress (MPa)	Change (%)	Number of Nodes
1	385.79	-	3850
2	753.38	64.535	10276
3	834.42	10.208	25516
4	850.47	1.9044	58218
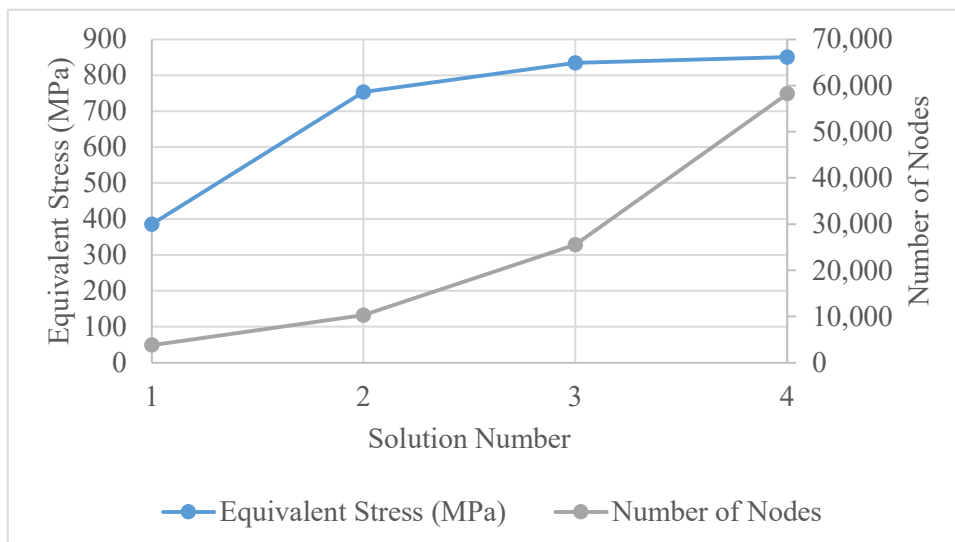
Figure 18. Equivalent Stress and Number of Nodes based on Ansys's Convergence Tool.

4.2 ANALSIS OF THE FILLED PIECE

4.2.1 Topology optimization

The next step was to understand the behavior of the topology optimization of the filled piece, thus obtaining a model to be followed when analyzing the subsequent topology optimizations and smoothing of the geometry. Due to the geometry of the filled piece in Fig. (10), the obtained values for stress were close to 20 MPa, returning no relevant results. This geometry is unsuitable for the problem due to its weight and shape, requiring structural optimization.

 For the topology optimization, two cases were run for load case one and load case two. The entire geometry was selected for optimization, but the boundary conditions were chosen as an exclusion zone to preserve the basic characteristics. Figure (19) shows the obtained results.
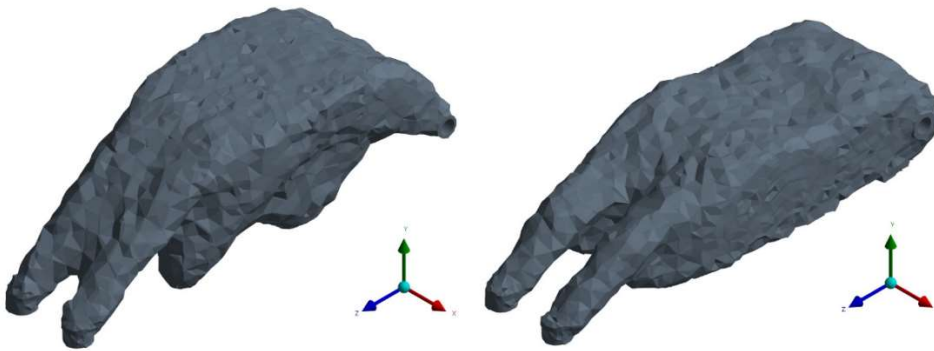
Figure 19. Topology optimization for load case numbers one and two of the filled pieces.

For the first case illustrated in the left, it is noticeable that the negative force in Y is acting on the upper fibers of the geometry, so the result is expected. The second case shown on the right shows a force with its largest negative component in Z and a small positive part in Y, so it corresponds to the result obtained of higher density of the piece in the central part of its length.

Figure (20) shows the critical parts that were removed and were taken into consideration for the next steps.

Figure 20. Curves shown in the optimization process for loading case one.

4.2.2 Importance of mesh quality

In order to further discuss the importance of mesh quality metrics, the optimization shown above was recreated using a low-quality mesh instead of the refined mesh before.

The mesh created used the default mesh settings Ansys would provide, also showing the necessity of learning meshing refinement to ensure the accuracy of results. The mesh used in Fig (21) had an average of Element Quality of approximately 0.50.
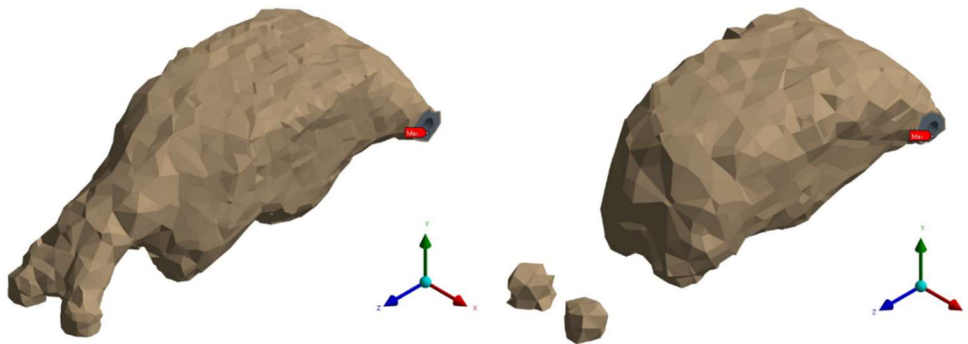
Figure 21. Topology optimization for both loading cases generated from a ow-quality mesh.

4.3 ANALYSIS OF THE GEOMETRY WITH THE ADDITION OF A CENTRAL CORE

4.3.1 Static structural analysis

The information obtained from the analyses performed with the filled part made it possible to notice the difference in stress reduction due to the presence of material in the hollowed upper part of the piece.

Using the geometries obtained in Fig (18), a new one was generated. Initially, a situation was considered where the central hollowed part of the geometry was filled, but as this result would also bring a heavy piece, a new approach was considered.

A central core was created instead of the full filling mentioned above, and the structural analyses were simulated. The piece used can be seen in Fig. (22), along with its stress values.
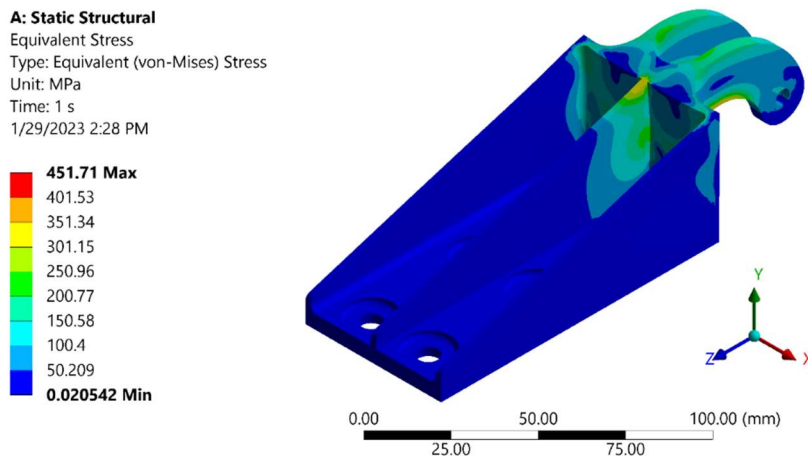
Figure 22. Equivalent (von Mises) Stress obtained for the support with the added core without optimization.

By adding the third core, a considerable improvement in the obtained stress can be noticed, which goes from 828 MPa to 452 MPa. An important consideration to be made is the presence of another high point of stress located at the upper junction of the added core with the structure.

4.3.2 Topology optimization

The result obtained by the optimization is shown in Fig. (23). The parameters used were 50% removal of geometry with the boundary conditions marked as an exclusion zone.
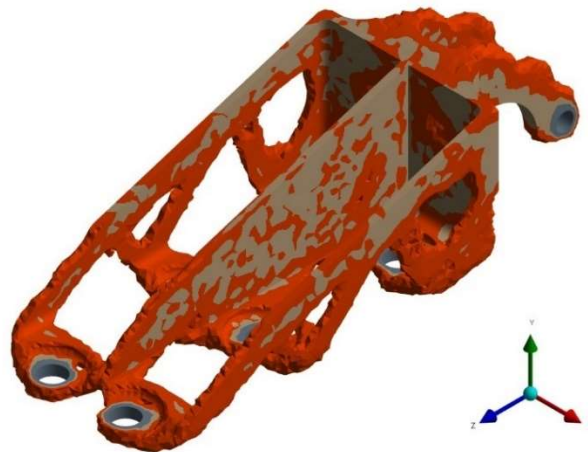
Figure 23. Topology optimization of the structure with the added central core.

During the post-processing analysis of the first few rounds of optimization, it was noticed that the optimization performed better when subjected to the efforts proposed by the first loading mode. The geometry of Fig. (22) returned satisfactory results, forming substructures similar to "fingers" on the side cores. This formation occurred mainly due to the concentration of efforts on the upper part, thus achieving a greater material removal. The piece's handle also deteriorated, showing that some work could be done in this region. Compared to the cycles present in Tomlin (2011), it is noticeable that the same change was adopted. Figure (24) displays the two cycles shown, where the second cycle was used in the final geometry, an improvement of the primary cycle.
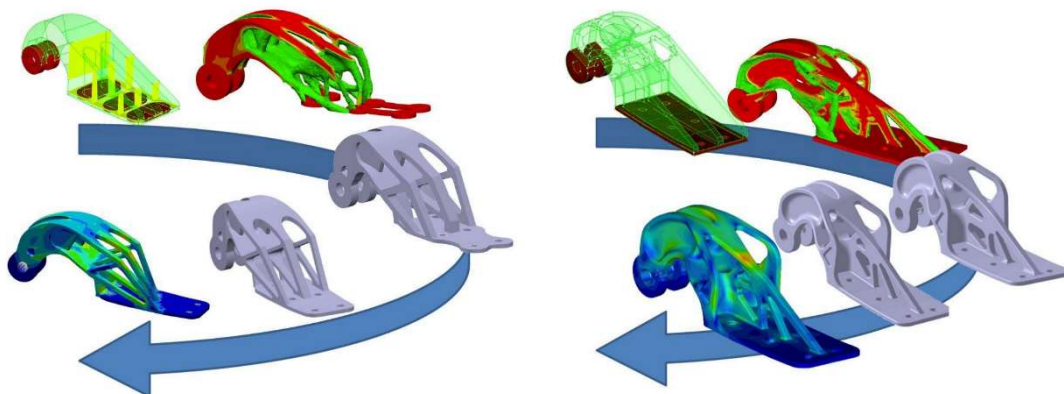
Figure 24. First (left) and second (right) adopted design cycle (TOMLIN, 2011).

Based on the collected results, it was possible to make a first optimized piece. Figure (25) shows the behavior of the structure when subjected to the main loading (two).
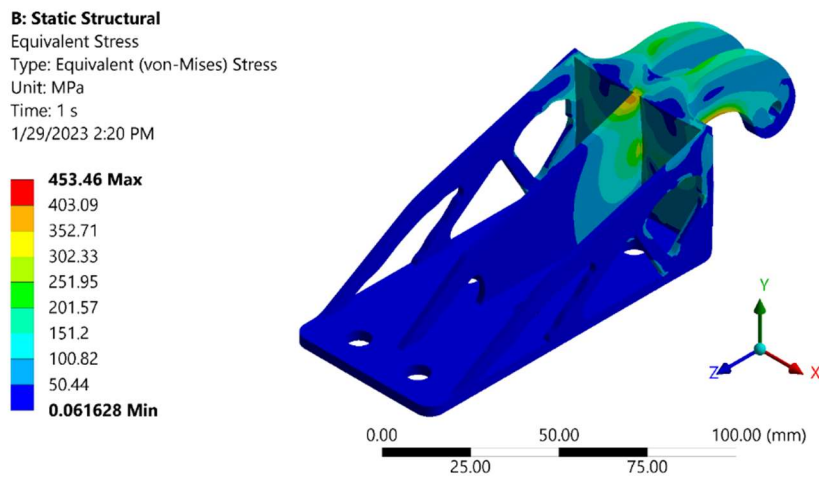
Figure 25. Static Structural Analysis of the first promising obtained optimization.

Figure (25) shows a new maximum stress of 453 MPa, a value like the pre-optimization analysis, with the maximum stress points concentrated in the same places. Despite the maintenance of the Von Mises stress, the volume of the piece did not show a considerable change with the value of 47,184 mm^3, a reduction of approximately 18%. This led to a new approach, redesigning the central fin and the two handles. The locations with the lowest stresses were also taken as possible locations for material removal. Finally, solutions were thought of that could reduce the high-stress point at the upper junction of the central core with the structure.

After analyzing the results for the Equivalent Stress, the geometry was placed for another optimization process for both loading cases. The results are shown in Fig. (26).
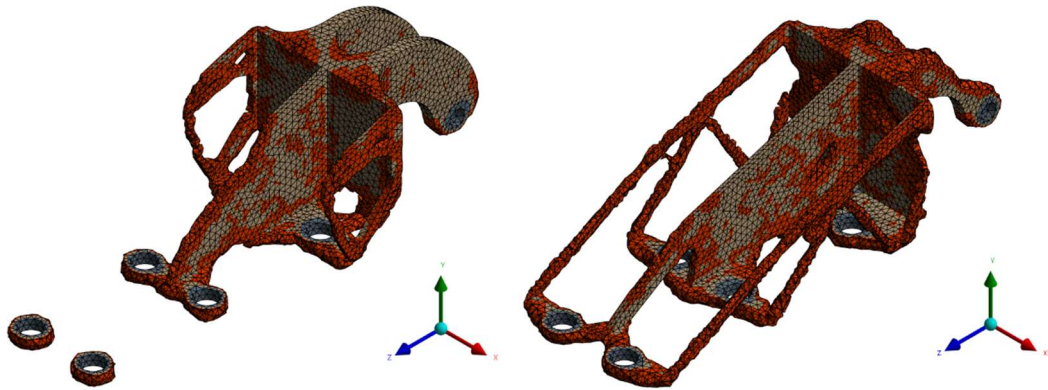
Figure 26. Optimization results for both loading cases.

It is noticeable on the left figure (loading case number 2) the maintenance of the handle and the removal of a considerable amount of mass on the side cores. That removal is justified by the lack of stress perceived in Fig. (24). The right figure shows some removal on the handles. However, for conservative purposes, by analyzing the presence of tensions of approximately 200 MPa, it was decided to keep the original geometry of them. Both figures show the removal of the base of the geometry, so another piece in which the base was going to be removed was considered.

4.4 FINAL GEOMETRY

4.4.1 Tomlin's final geometry

The final geometry obtained by Tomlin derives from the second project cycle shown in Fig. (23). The results will be shared here to serve as a comparison model for the conclusion of this thesis.

Figure (27) shows the obtained result.
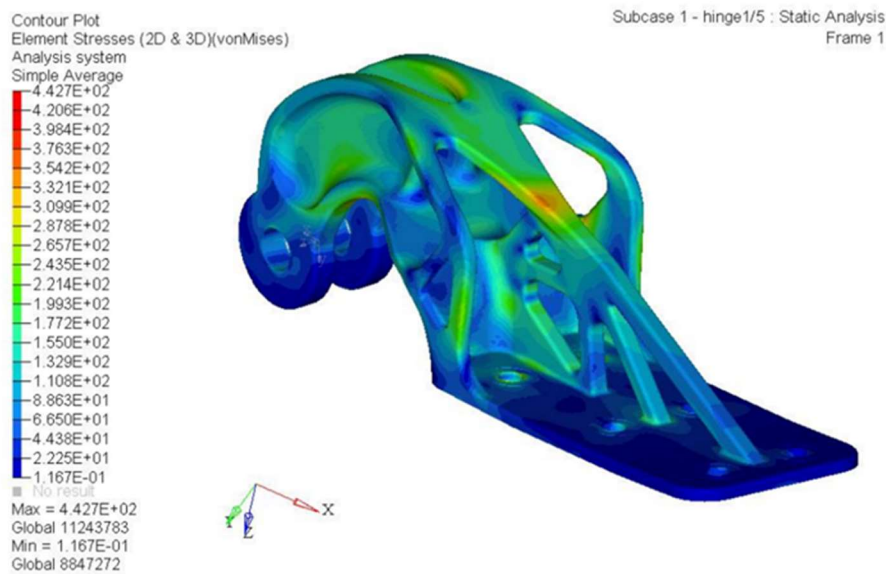
Figure 27. FEA of hinge design (TOMLIN, 2011).

The Equivalent Stress is set at a maximum of 442.7 MPa, less than half of the initial one. The mass sets at a 63% reduction, with the new geometry weighing 326 g.

4.4.2 Created final geometry design

The final geometry was based on the results for the topology optimization shown in Fig. (26). As mentioned above the base was kept for conservative purposes, therefore most of the mass had to be removed from the three cores. Both side cores had the two front joints connected to the cylindrical support removed, justified by the low tensions shown in Fig. (25) and the optimization for loading case 1 on Fig. (26).

Although the optimization showed no progress for the central core, cavities were added after analyzing the results on Fig. (25).

Figure (28) shows the correlation between the faceted geometry and the newly designed one.

Figure 28. Comparison between optimization results from load case 1 and the final obtained geometry.

4.4.3 Mesh metrics

The same comparison between mesh maximum size, element quality and von Mises's tension made for the original geometry were repeated for the final optimized geometry. The previously stipulated minimum average mesh element quality of 0.75 was also used. The results obtained from the comparison can be visualized in Tab (8).

Table 8 - Mesh metrics obtained for the final geometry.

Mesh Metric	Mesh Average	Standard Deviation
Element Quality	0.8147	0.1046
Skewness	0.2598	0.1406
Jacobian Ratio	0.9935	0.0254
Aspect Ratio	1.9215	0.5874

Figure (29) shows the mesh created for the subsequent analyses generated.
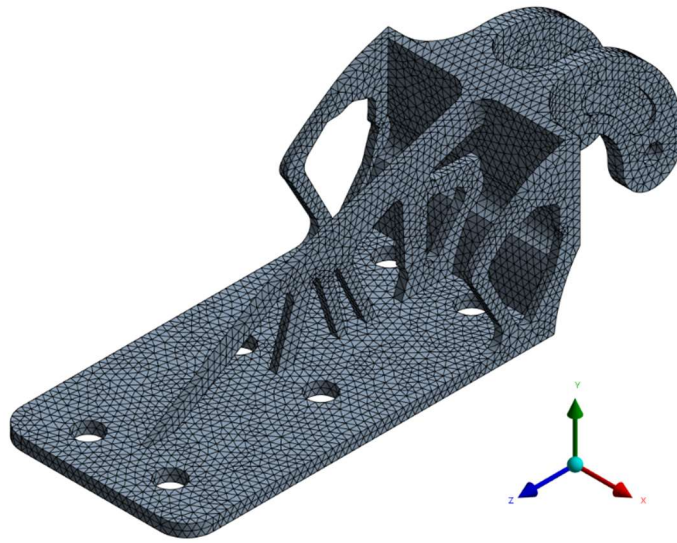
Figure 29. Generated mesh for final geometry.

4.4.4 Static structural analysis

With the afore mentioned boundary conditions applied to the model, Fig. (30) shows the obtained results.
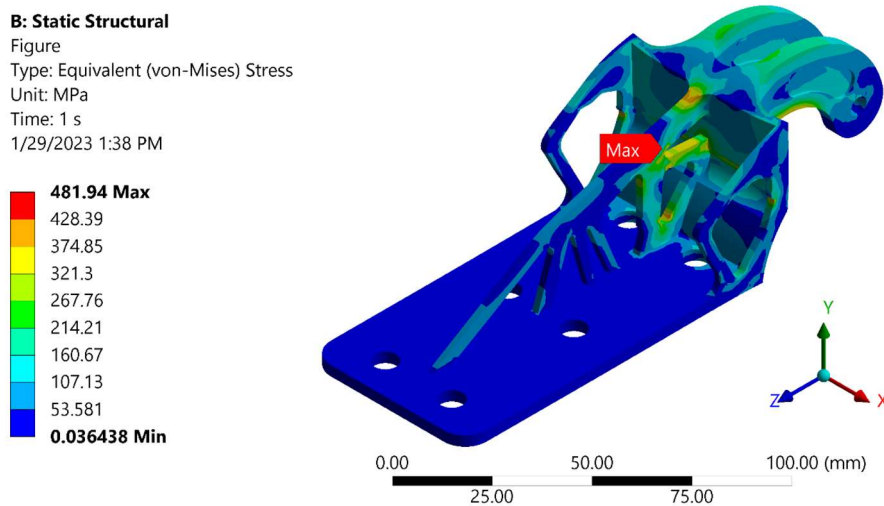
Figure 30. Isometric view of the Equivalent (von Mises) Stress for final optimized support.

It is possible to notice that the maximum stress present in the structure reaches the value of 482 MPa, well below the 800 MPa obtained for the original piece. The peak values are present near the two upper junctions of the central core with the

handle. Figure (30) also informs us about maximum stress points in the connections between the handle and the bottom of the geometry. The safety coefficient for Von Mises is now 1.9, well above the previously found one.

The new mass of the piece is 188.14 g, below the previous one of 440 g.

4.4.4.1 Mesh convergence

The Mesh Convergence tool was used to check the results the same way as for the initial piece. The percentage used as reference was also 3%, meaning that the program will be satisfied if the new value has a change of less than 3%.

Table (9) and Fig. (31) show the obtained results.

Table 9 – Convergence tool data from initial geometry analysis for the final geometry.

Solution Number	Equivalent Stress (Mpa)	Change (%)	Nodes
1	390.32	-	5,508
2	491.39	22.925	15,516
3	505.13	2.7584	39,281
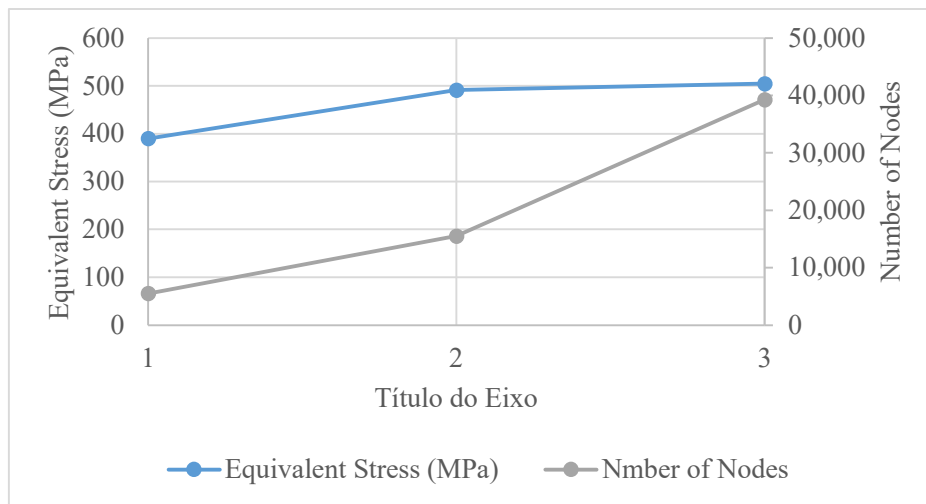
Figure 31. Equivalent Stress and Number of Nodes based on Ansys's convergence tool for the final geometry.

4.4.4.2 Smoothened geometry

Given that geometries to be analyzed must be simplified, final modifications were made to eliminate the sharp corners present and adding concurrences. Figure (32) shows the result.
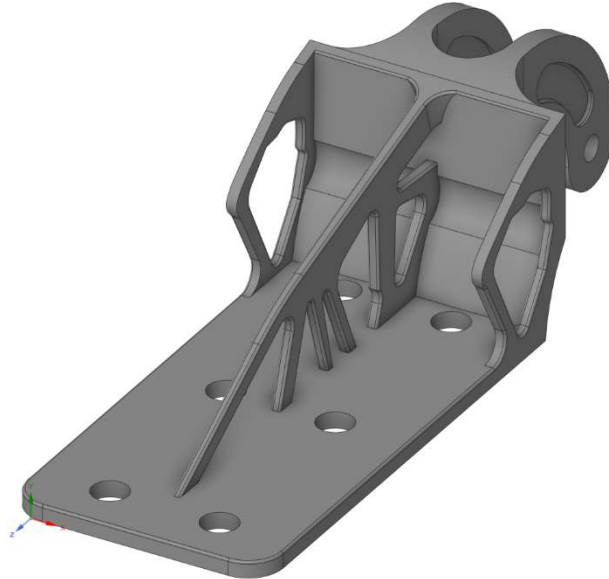
Figure 32. Final smoothened piece obtained.

4.4.4.3 Final geometry comparison

At last, it is important to bring a comparison between the two final geometries, the one generated from this work and the one presented by Tomlin & Meyer. Figure (33) shows the comparison.
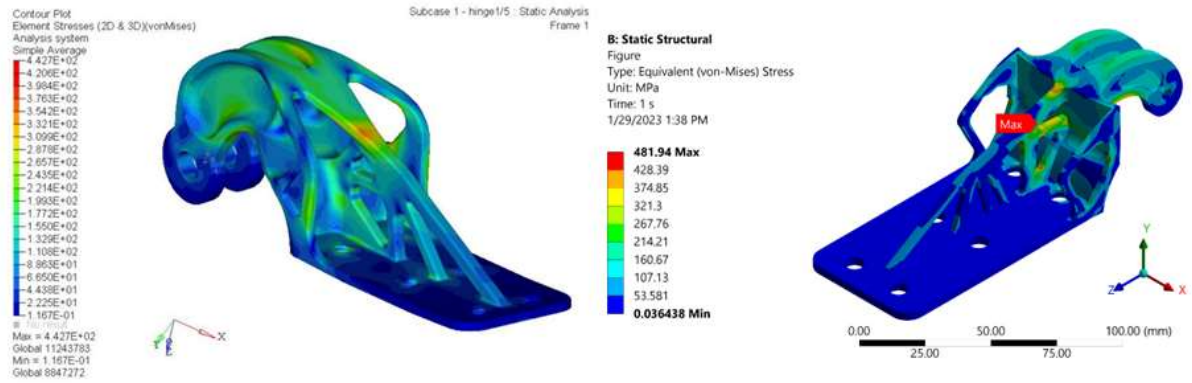
Figure 33. Final geometries obtained by Tomlin & Meyer and the authors.

As noted before a great improvement has been made in in their tension field. The result is a much more requested geometry, especially in areas above the bottom part, where the supports are located. Both maximum values for von Mises are between 445 MPa and 485 MPa, a considerable reduction from the initial geometries.

5 CONCLUSION

The project developed in this thesis aimed to create a model for reproducing the structural part optimization method used in the aerospace industry, based on a study by Tomlin and Meyer. Considering the differences between the original project and the one described here, a comparison was made based on the results obtained. As this is a topological optimization analysis, the focus was on reducing the mass and reducing the maximum stresses suffered by the new part compared to the initial part.

In the original article (TOMLIN, 2011), a final comparison of the results shows a reduction in weight from 918 g to 326 g (64 % reduction) and a reduction in the maximum Von Mises stress from 835.6 MPa to 442.7 MPa (47 % reduction). In addition, it is possible to observe a more homogeneous distribution of stresses, showing a better utilization of the material.

Upon comparing the data obtained in this dissertation, a reduction in mass from 440.33 g to 188.14 g (57 % reduction) and a corresponding reduction in the maximum Von Mises stress from 828.02 MPa to 482 MPa (41 % reduction) is observed. It is also noticeable from Figure 41 that the same homogenization of the stress field is present, showing an also more efficient geometry.

Although the execution was on a small part with a very small total weight when compared to the weight of the entire aircraft, the application of topological optimization analysis proved to be a very feasible option when applied to parts with potential for improvements, which, as seen, when combined with the right material choice can lead to mass reductions of more than half of the original structure. Common sense should be used during the analyses, always paying attention to design requirements and always prioritizing safety.

5.1 SUGGESTIONS FOR FUTURE PROJECTS

This work has potential for further expansion in multiple ways. Future research on the topological optimization analysis of aerospace parts could include the fabrication and testing of the resulting object in the laboratory. This would involve manufacturing the optimized part using the chosen material and manufacturing method, and subjecting it to various mechanical and laboratory tests to validate the results of the numerical simulations.

One possible test that could be performed is tensile testing, which involves applying a uniaxial force to the part to measure its tensile strength, yield strength, and other mechanical properties. This test would provide valuable information on the mechanical behavior of the part and its ability to withstand loads.

Another potential test is fatigue testing, which involves applying cyclic loads to the part to simulate the effects of repeated loading and unloading over time. This test would provide insight into the durability and longevity of the part under real-world operating conditions.

Crack growth analysis could also be performed to evaluate the part's ability to resist the growth of cracks and fractures. This test involves introducing a crack into the part and measuring the rate of crack growth under various loads and conditions.

Finally, additive manufacturing simulations could be performed to evaluate the manufacturability of the optimized part using 3D printing or other additive manufacturing methods. This would involve simulating the printing process to identify potential issues and optimize the design for additive manufacturing.

Overall, the fabrication and testing of the optimized part would provide valuable insights into the real-world performance and manufacturability of the part, and could lead to further improvements and refinements in the topological optimization analysis process.

BIBLIOGRAPHY

ADDERE. Titanium in the Automotive Industry. 2021. Retrieved from: https://www.addere.com/titanium-in-the#:~:text=Brake%20calipers%2C%20engine%20valves%2C%20tire,in%20the%20parts'%20overall%20weight. Accessed in: 12 Jan. 2023.

ANA (Japan). An action towards "zero" CO_2 emissions: weight reduction of in-flight car. Weight reduction of in-flight car. 2021. Retrieved from: https://www.ana.co.jp/en/jp/brand/ana-future-promise/co2-reduction/2021-08-04-02/. Accessed in: 16 ago. 2021.

ANSYS. Adaptive convergence. 2022. Retrieved from: https://ansyshelp.ansys.com/account/securedreturnurl=/Views/Secured/corp/v231/en/wb_sim/ds_Convergence.html Accessed in: 12 Jul. 2022.

ANSYS. Element quality. 2022. Retrieved from: https://ansyshelp.ansys.com/account/secured?returnurl=/Views/Secured/corp/v222/en/wb_msh/msh_Element_Quality_Metric.html. Accessed in: 12 Jul. 2022.

ANSYS. Element Solid 187. 2023 Retrieved from: https://ansyshelp.ansys.com/account/secured?returnurl=/Views/Secured/corp/v231/en/ans_elem/Hlp_E_SOLID187.html Accessed in 05 Jan. 2023.

ANSYS. Jacobian ratio. 2023. Retrieved from: https://ansyshelp.ansys.com/account/secured?returnurl=/Views/Secured/corp/v231/en/wb_msh/msh_jacobian_ratio.html?q=jacobian%20ratio. Accessed in: 07 Jan. 2023.

BELYTSCHKO, Ted; LIU, Wing Kam; MORAN, Brian P.. Nonlinear Finite Elements for Continua and Structures. 2. ed. New York: John Wiley & Sons, 2014. 804 p.

BENDSOE, M.P; SIGMUND, O.. Topology optimization: theory, methods and aplications. 2. ed. Berlim: Springer, 2003.

BENDSØE, Martin Philip; KIKUCHI, Noboru. Generating optimal topologies in structural design using a homogenization method. Computer Methods In Applied Mechanics And Engineering, [S.L.], v. 71, n. 2, p. 197-224, Nov. 1988. Elsevier BV. http://dx.doi.org/10.1016/0045-7825(88)90086-2.

COOK, Robert Davis; MALKUS, David S.; PLESHA, Michael E.. Concepts and Applications of Finite Element Analysis. 4. ed. New York: John Wiley & Sons, 2001. 719 p.

COTTRELL, J. Austin; HUGHES, Thomas J. R; BAZILEVS, Yuri. Isogeometric Analysis: Toward Integration of CAD and FEA. Eindhoven: John Wiley & Sons, 2009. 335 p.

FREY, Pascal Jean; GEORGE, Paul-Louis. Mesh Generation. 2. ed. New York: Wiley, 2008. 848 p.

IATA (Montreal). Net-Zero Carbon Emissions by 2050. 2021. Retrieved from: https://www.iata.org/en/pressroom/pressroom-archive/2021-releases/2021-10-04-03/. Accessed in: 05 jan. 2023.

PRIOR, Madelaine. Boeing and Titomic Partner to Expand Use of Titanium in Aerospace Industry. 2022. Retrieved from: https://www.3dnatives.com/en/boeing-titomic-expand-titanium-aerospace-industry-060120214/. Accessed in: 12 Jan. 2023.

PULLAN, Amy. Titanium Powder used to 3D print automotive parts. 2013. Retrieved from: https://www.sheffield.ac.uk/news/nr/3d-printing-titanium-1.332731. Accessed in: 12 Jan. 2023.

RAO, Singiresu S.. The Finite Element Method in Engineering. 5. ed. Oxford: Butterworth-Heinemann, 2010. 710 p.

REDDY, J.N.. An introduction to the finite element method. 3. ed. Department of Mechanical Engineering Texas A&M University: McGraw Hill, 2006. 772 p.

SEABRA, Miguel; AZEVEDO, José; ARAðJO, Aurélio; REIS, Luís; PINTO, Elodie; ALVES, Nuno; SANTOS, Rui; MORTÁGUA, João Pedro. Selective laser melting (SLM) and topology optimization for lighter aerospace components. Procedia Structural Integrity, [S.L.], v. 1, p. 289-296, 2016. Elsevier BV. http://dx.doi.org/10.1016/j.prostr.2016.02.039.

SIGMUND, Ole; MAUTE, Kurt. Topology optimization approaches. Structural And Multidisciplinary Optimization, [S.L.], v. 48, n. 6, p. 1031-1055, 21 ago. 2013. Springer Science and Business Media LLC. http://dx.doi.org/10.1007/s00158-013-0978-6.

TOMLIN, J. M. M. Topology optimization of an additive layer manufactured (ALM) aerospace part. 2011.

TABERNIER, Laurent; DERANSY, Robin; RUTHERFORD, Dan. Economic Fuel Tankering: A Threat to Aviation Decarbonisation. Montreal: Icao, 2022.

TOMLIN, Matthew; MEYER, Jonathan. Topology Optimization of an Additive Layer Manufactured (ALM) Aerospace Part. Altair Engineering: Altair, 2011. 9 p.

U.S. TITANIUM INDUSTRY INC. (United States). Titanium Alloys - Ti6Al4V Grade 5. 2002. Disponível em: https://www.azom.com/article.aspx?ArticleID=1547. Accessed in: 26 Nov. 2022.

ZIENKIEWICS, O.C.; TAYLOR, R. L.; ZHU, J.Z.. The finite element method: its basis & fundamentals. 7. ed. Oxford: Butterworth-Heinemann, 2013. 756 p.